GMR
The Original

TERMINAL HEAT STRESS DIFFERENTIALLY MODULATES ROOT ARCHITECTURE, CARBOHYDRATE STATUS AND NODULATION IN LENTIL (*LENS CULINARIS* MEDIK.): IMPLICATIONS FOR IDENTIFYING HEAT-RESILIENT GENOTYPES

Jyostnarani Pradhan[1], Chandani Kumari[1], Kshirod Chandra Sahoo[2], Hemlata Singh[1*], Swati Bhimrao Gaikwad[1], Shiv Nath Suman[2], Ravi Prakash[1], Kartik Pramanik[3*]

[1]Department of Plant Physiology and Biochemistry, College of Basic Sciences and Humanities, Dr. Rajendra Prasad Central Agricultural University, Pusa, Samastipur-848125, Bihar, India
[2]Department of Soil Science, Post Graduate College of Agriculture, Dr. Rajendra Prasad Central Agricultural University, Pusa, Samastipur-848125, Bihar, India
[3]Department of Horticulture, M. S. Swaminathan School of Agriculture, Centurion University of Technology and Management, R. Sitapur, Paralakhemundi, Gajapati, Odisha-761211, India
***Correspondance**: Hemlata Singh, hemlata@rpcau.ac.in

ABSTRACT
Lentil is an important pulse crop which also provides biological nitrogen fixation advantage to cropping systems, but lentil sown late can suffer 36-59% loss in yield due to terminal heat stress, and India, the biggest producer and consumer of lentil, has to import about 1.2 million tonnes of lentil each year. Responses of lentil to shoot-level heat exposure have been investigated extensively, but root-level responses have not been investigated as much and there is a lack of systematic evaluation of root architecture, carbohydrate status, and nodulation across genotypes. A total of 28 lentil genotype were evaluated to determine their root, carbohydrate and nodulation responses under control, mid-late and late sowing to increase the amount of heat stress at the end of the season. Delayed sowing caused a drastic reduction in root volume (81.5%), root diameter (70.0%) and nodule number (72.3%), and moderate reduction in carbohydrate content (13.7%) with an increase in root length, suggesting a compensatory elongation response, root surface area was fairly stable. There was significant variation in each genotype for each of the traits, indicating different heat adaptation strategies. Root volume, diameter and nodule number were found to be correlated and grouped together as a "root vigor – nodulation" complex (PC1 31.2%) against which root elongation was opposed, and with surface area and carbohydrate content as a separate complex (PC2 23.9%), accounting for 55.1% of the variance. Nodule number was the most important direct factor in the path analysis of root biomass (0.49), mainly through root volume which is the most useful indirect selection criterion for breeding heat-tolerant lentil cultivars.

KEYWORDS: delayed sowing, root architecture, root nodulation, root carbohydrates, correlation, heat tolerance.

1. INTRODUCTION

Lentil (*Lens culinaris* Medik.) is one of the nutritionally valuable pulse crops and is also suitable for sustainable agriculture as it provides biological nitrogen fixation to the soil; however, it is experiencing a decline in its yield because of early warm weather during its terminal growth stage. The high temperature stress can decrease lentil yield by 36- 59%. India is the largest producer as well as consumer of lentil; however to fulfill the demand the country imports about 1.2 MT from countries like Canada and Australia. This indicates an urgent need of high temperature tolerant genotype in this crop to meet the demand. As with above-ground tissues, plant roots can be subjected to stressful high temperatures that can limit whole-plant function and decrease crop productivity. In addition, root heat stress events will get more frequent, longer and more intense with impending climate change. In comparison to shoot function, especially photosynthesis, much less is known regarding heat stress and roots. High temperature resulted in a significant reduction in both micronutrients (Sita et al., 2018). In many crops, it has been reported that a moderately high temperature decreased root uptake of nutrients (Choukri et al., 2022). Sowing date has a significant effect on temperature regimes experienced by lentil crops. Lentil crops sown in the Indo-Gangetic Plains (IGP) are usually early sown (October–November) and do not experience terminal heat stress, but late sown crops (December–January) experience progressively higher temperatures at the critical vegetative and reproductive stages with maximum temperatures often exceeding 30–35 °C during pod filling (Aktar-Uz-Zaman et al., 2022).

Under heat stress, drought-induced decreases in root biomass and changes to root morphology may also affect water and nutrient acquisition (Lynch, 2022), adding to the effects of high temperatures on the shoot system (Luo et al., 2020). The biological nitrogen fixation by the rhizobium in legumes is very sensitive to heat stress

and low root nodule numbers and function may have a significant impact on plant nitrogen status (Serova et al., 2023).

Although the agronomic relevance of lentil is high, the effect of heat stress due to variation of sowing time is a problem and a systematic evaluation of root traits under this stress condition by different sowing dates is scanty. Root-level responses are under-represented in the literature of heat stress in lentils and most studies have concentrated on above-ground phenotyping (canopy temperature, yield attributes, chlorophyll content). Genotypic variation in root morphological and biochemical traits in heat stress condition would be useful to understand for selection of heat stress ideotype from lentil germplasm. The present study is designed to explore the genotypic variability in the root characteristics, accumulation of carbohydrates and nodulation under heat stress due to delayed sowing and to determine heat-adaptive traits.

2. MATERIALS AND METHODS

The experiment was carried out at the Research Farm of Rajendra Prasad Central Agricultural University (RPCAU), Pusa, Samastipur, Bihar, India (altitude 52 m above mean sea level, 25°58′N, 85°40′E). Twenty eight lentil genotypes evaluated in the study and were designated as G1 to G28 as follows: G1 (IPL 329), G2 (IPL 225), G3 (IPL 220), G4 (IPL 406), G5 (IPL 321), G6 (IPL 526), G7 (IPL 230), G8 (IPL 315), G9 (IPL 81), G10 (IPL 316), G11 (IPL 341), G12 (IPL 534), G13 (PANT L 9), G14 (PANT 117), G15 (PA), G16 (PL 9), G17 (PSL 9), G18 (DPL 15), G19 (DPL 62), G20 (KSL 218), G21 (HUL 57), G22 (VL 148), G23 (L 4727), G24 (L 4062), G25 (L-9-12), G26 (LL-1698), G27 (LL-1694), and G28 (LL-1641). These were raised in the seed farm RPCAU and ICAR-IIPR Kanpur after their agro-morphological characterization. The experiment was designed in two factor completely randomized design (CRD) with three replications. Three sowing dates were used in Factor A; E1 (timely sown 1st week of November), E2 (mid-late sown 3rd week of November) and E3 (late sown 1st week of December). The effects of sowing delays were observed as a higher heat stress affecting plants as the sowing date was postponed; the maximum temperatures were higher in E3 than in all other sowing dates. There were 28 genotypes (G1–G28) in factor B. All treatments were carried out in accordance with the recommended package of agronomic practices. At the flowering stage (50% flowering), root samples were taken from three plants per treatment. The roots were thoroughly cleaned of soil particles and subjected to morphological and biochemical analyses right away. After scanning the roots, at 800 dpi on an Epson Expression 11000XL flatbed scanner, root morphological traits such as root surface area (cm^2), root length (cm), root volume (cm^3) and root diameter (mm) were measured using the WinRHIZO image analysis system (Regent Instruments, Canada). The size of root nodules was measured manually (number $plant^{-1}$), and the quantity of carbohydrates in root nodules was measured by the anthrone method (Bader et al., 2024) (mg g^{-1} DW). Each measurement was repeated three times. Analysis of variance (ANOVA) was used to analyze the data, as designed in the CRD with factorial arrangement in R software (v4.3.0). The base graphics package in R was used to create box plots to show the distribution of trait values for sowing date (Factor A) and genotype (Factor B). Significant difference was considered at $p \leq 0.05$ level. Where appropriate, means were compared with Tukey's HSD post-hoc test.

3. Results

	SoV	DF	RSA	RL	RV	RSD	RN	CHO	RB
1	Factor A	2	7666.98**	48077.56**	5933.69**	522.19**	6638.01**	3.79**	1.26**
2	Factor B	27	5456.31**	10473.88**	328.86**	27.32**	30.83**	30.20**	0.11**
3	AxB	54	3879.19**	12453.21**	282.76**	26.05**	31.91**	2.41**	0.04**
4	Error	168	81.60	65.19	0.58	0.04	1.88	0.10	0.00

Table 1: Treatment and Error Mean Squares (ANOVA) SoV = Source of Variation, DF = Degrees of Freedom; Mean squares are provided for each character; * indicates significance at 5% level, ** indicates significance at 1% level, NS indicates non-significance.

The main effects of environment (sowing-date-induced temperature regime; Factor A), genotype (Factor B) and the A × B interaction effects were highly significant at $p < 0.001$ for all seven traits (Table 1), namely root surface area (RSA), root length (RL), root volume (RV), root surface diameter (RSD), root nodule number (RN), root total carbohydrate (CHO), and root biomass (RB). The mean squares for most traits under Factor A (environment) were generally higher than under Factor B (genotype) and Factor A × B (genotype × environment), suggesting that the role of environment was predominant over the effects of genotype in the expression of root/nodulation related traits (e.g., RL: 48,077.56 vs. 10,473.88 and 12,453.21, respectively). The large G×E interaction for all traits indicates that the temperature levels did not result in a similar effect on the genotypes and that simple effects analysis is warranted (Tables 2–4).

	RSA	RL	RV	RSD	RN	CHO	RB
E1	244.33 ± 40.57[a]	88.50 ± 53.54[c]	18.86 ± 16.19[a]	6.50 ± 4.33[a]	24.07 ± 5.18[a]	2.77 ± 1.94[a]	0.50 ± 0.13[a]

	RSA	RL	RV	RSD	RN	CHO	RB
E2	226.04 ± 33.51^{c}	120.15 ± 64.30^{b}	5.28 ± 4.60^{b}	2.45 ± 1.85^{b}	12.23 ± 2.41^{b}	2.42 ± 1.92^{b}	0.37 ± 0.12^{b}
E3	239.98 ± 41.17^{b}	135.40 ± 68.12^{a}	3.48 ± 2.99^{c}	1.95 ± 1.94^{c}	6.67 ± 1.38^{c}	2.39 ± 2.04^{b}	0.26 ± 0.18^{c}
F stat	93.95**	737.55**	10185.40**	12248.62**	3536.53**	38.51**	396494.00**
p value	< 0.001						
MSE	81.60	65.19	0.58	0.04	1.88	0.10	0.00
SE(m)	0.99	0.88	0.08	0.02	0.15	0.03	0.00
SE(d)	1.39	1.25	0.12	0.03	0.21	0.05	0
CV(%)	3.82	7.04	8.29	5.69	9.57	12.43	0.48
Cohen's F	1.06	2.96	11.01	12.08	6.49	0.68	68.70

Table 2: Detailed tabular representation with Multiple comparisons for Factor A . Cell values represent mean ± SDSD. Transformed means are shown in parentheses; Treatments with the same letter grouping are not significantly different; * indicates significance at 5% level; ** indicates significance at 1% level, NS indicates non-significance; MSE and CV (%) are common for this experiment.

All traits were significantly influenced by environment ($p < 0.001$; Table 2). Timely-sown environment (E1) had the largest root volume (18.86 cm³), root surface diameter (6.50), number of root nodules (24.07), total root carbohydrates (2.77) and biomass (0.50) whereas the delayed, heat-stressed environments E2 and E3 had progressively reduced values for all parameters. The reduction in the number of nodules formed was particularly strong, from 24.07 with E1 to 6.67 with E3 ($F = 3536.53$, $p < 0.001$); heat stress had been shown to reduce rhizobial nodulation and symbiotic nitrogen fixation in legume–rhizobium symbioses. However, root length had the opposite response, increasing from 88.50 cm under E1 to 135.40 cm under E3, suggesting a compensatory reaction in increasing root length under E1 and E3 to find a larger soil volume to grow in when nodulation and root volume decreased. The root surface area was maximum in E1 (244.33) and minimum in E2 (226.04) (a pattern which was non-monotonic, but is discussed further below) as compared to the other treatments. The coefficient of variation (0.48–12.43%) and Cohen's f (1.06–68.70%) showed good experimental precision and environment had the highest practical effect size for root biomass.

	RSA	RL	RV	RSD	RN	CHO	RB
G1	282.16 ± 23.49^{a}	183.68 ± 70.44^{a}	3.67 ± 3.52^{p}	1.44 ± 0.66^{op}	13.67 ± 8.92^{hi}	1.94 ± 0.45^{gh}	0.15 ± 0.12^{y}
G2	216.05 ± 46.44^{nop}	128.04 ± 33.15^{de}	3.95 ± 0.39^{op}	2.04 ± 0.22^{m}	15.11 ± 9.91^{cdefgh}	0.47 ± 0.22^{op}	0.41 ± 0.24^{j}
G3	242.20 ± 22.66^{hij}	179.16 ± 26.25^{ab}	2.58 ± 1.28^{q}	1.32 ± 0.29^{p}	11.78 ± 4.38^{jk}	4.97 ± 0.09^{c}	0.43 ± 0.24^{h}
G4	257.11 ± 55.22^{def}	90.42 ± 40.22^{l}	17.98 ± 23.39^{d}	1.66 ± 0.89^{n}	13.22 ± 5.52^{i}	1.56 ± 0.03^{ijk}	0.36 ± 0.11^{o}
G5	210.12 ± 45.10^{pq}	112.23 ± 73.10^{ghi}	19.90 ± 21.02^{c}	7.25 ± 7.75^{a}	16.33 ± 9.43^{abc}	1.55 ± 0.03^{ijk}	0.48 ± 0.15^{e}
G6	255.41 ± 14.90^{ef}	114.40 ± 41.96^{ghi}	11.30 ± 12.15^{f}	3.79 ± 2.94^{gh}	16.11 ± 9.92^{abcd}	1.42 ± 0.29^{jk}	0.28 ± 0.16^{t}
G7	274.07 ± 57.61^{ab}	143.27 ± 116.35^{c}	26.25 ± 30.27^{a}	5.96 ± 5.35^{c}	16.67 ± 9.33^{ab}	7.79 ± 0.69^{a}	0.36 ± 0.18^{o}
G8	267.15 ± 24.12^{bc}	113.55 ± 101.08^{ghi}	8.80 ± 3.59^{i}	2.50 ± 1.53^{kl}	13.78 ± 10.50^{ghi}	6.84 ± 0.04^{b}	0.40 ± 0.09^{k}
G9	237.69 ± 13.88^{ijk}	110.58 ± 24.89^{hi}	3.33 ± 3.77^{p}	1.58 ± 0.99^{no}	14.00 ± 7.87^{ghi}	0.99 ± 0.11^{lm}	0.26 ± 0.11^{v}
G10	228.78 ± 17.21^{klm}	101.76 ± 37.60^{jk}	6.08 ± 8.00^{kl}	2.63 ± 2.34^{k}	14.33 ± 10.17^{efghi}	2.18 ± 0.39^{g}	0.27 ± 0.09^{u}
G11	260.29 ± 27.88^{cde}	82.04 ± 51.92^{mno}	21.25 ± 18.30^{b}	4.93 ± 5.73^{e}	15.22 ± 9.86^{bcdefg}	1.82 ± 0.35^{hi}	0.53 ± 0.27^{b}
G12	244.64 ± 14.67^{ghij}	129.09 ± 72.42^{de}	6.52 ± 7.49^{k}	2.34 ± 1.83^{l}	15.78 ± 8.61^{abcde}	3.00 ± 2.09^{ef}	0.29 ± 0.07^{r}
G13	220.52 ± 13.92^{mno}	58.43 ± 32.87^{q}	14.53 ± 14.90^{e}	3.88 ± 1.96^{gh}	14.11 ± 8.85^{fghi}	4.74 ± 1.91^{c}	0.29 ± 0.19^{s}
G14	252.38 ± 21.11^{efg}	99.45 ± 51.61^{k}	10.77 ± 14.75^{fg}	3.39 ± 3.84^{i}	15.11 ± 9.47^{cdefgh}	1.84 ± 0.74^{hi}	0.32 ± 0.13^{p}

	RSA	RL	RV	RSD	RN	CHO	RB
G15	236.14 ± 39.60^{jk}	75.23 ± 25.19^{o}	7.74 ± 6.93^{j}	3.76 ± 2.49^{gh}	15.56 ± 9.22^{bcdef}	1.00 ± 0.15^{lm}	0.38 ± 0.19^{l}
G16	211.51 ± 22.35^{opq}	82.62 ± 24.47^{lmno}	6.40 ± 5.20^{k}	2.70 ± 1.40^{k}	15.67 ± 11.27^{bcde}	0.86 ± 0.28^{mn}	0.24 ± 0.09^{w}
G17	245.67 ± 68.15^{ghi}	119.44 ± 57.49^{fg}	4.57 ± 0.73^{no}	4.35 ± 3.12^{f}	17.22 ± 9.43^{a}	1.79 ± 1.57^{hi}	0.52 ± 0.01^{c}
G18	231.61 ± 11.18^{kl}	129.36 ± 37.79^{de}	2.29 ± 0.54^{q}	1.53 ± 0.37^{no}	16.11 ± 9.53^{abcd}	3.22 ± 1.61^{e}	0.53 ± 0.12^{b}
G19	222.62 ± 40.25^{lmn}	85.92 ± 16.55^{lmn}	5.38 ± 2.72^{lm}	3.01 ± 2.00^{j}	10.44 ± 4.69^{k}	0.67 ± 0.13^{no}	0.42 ± 0.16^{i}
G20	224.36 ± 19.88^{lmn}	117.52 ± 60.50^{fgh}	3.98 ± 2.76^{op}	2.50 ± 2.00^{kl}	14.67 ± 6.56^{defghi}	2.71 ± 0.15^{f}	0.47 ± 0.10^{f}
G21	268.02 ± 40.48^{bc}	88.44 ± 68.43^{lm}	7.94 ± 6.01^{j}	6.75 ± 4.53^{b}	15.22 ± 8.61^{bcdefg}	3.73 ± 0.14^{d}	0.51 ± 0.14^{d}
G22	264.85 ± 39.85^{cd}	80.00 ± 54.55^{no}	13.85 ± 7.62^{e}	7.41 ± 5.20^{a}	15.22 ± 8.30^{bcdefg}	3.71 ± 0.17^{d}	0.37 ± 0.06^{n}
G23	249.85 ± 31.19^{fgh}	175.39 ± 67.62^{b}	10.13 ± 6.01^{gh}	5.03 ± 3.46^{e}	14.78 ± 7.01^{defgh}	1.83 ± 1.43^{hi}	0.32 ± 0.10^{p}
G24	225.72 ± 22.87^{lm}	178.44 ± 90.68^{ab}	9.87 ± 5.12^{h}	3.96 ± 2.61^{g}	11.89 ± 4.31^{j}	3.93 ± 0.14^{d}	0.19 ± 0.13^{x}
G25	199.02 ± 10.23^{r}	123.29 ± 42.11^{ef}	5.13 ± 4.92^{mn}	3.07 ± 2.28^{j}	10.44 ± 3.21^{k}	2.83 ± 1.39^{f}	0.58 ± 0.10^{a}
G26	205.29 ± 26.80^{qr}	108.06 ± 22.41^{ij}	7.79 ± 6.57^{j}	3.67 ± 2.80^{h}	11.67 ± 2.65^{jk}	1.71 ± 0.35^{hij}	0.31 ± 0.10^{q}
G27	211.75 ± 29.01^{opq}	134.14 ± 97.07^{d}	9.09 ± 8.07^{i}	3.88 ± 3.81^{gh}	11.78 ± 5.67^{jk}	1.26 ± 0.47^{kl}	0.46 ± 0.11^{g}
G28	185.02 ± 5.05^{s}	67.13 ± 49.51^{p}	6.72 ± 6.04^{k}	5.35 ± 4.99^{d}	15.11 ± 8.96^{cdefgh}	0.34 ± 0.11^{p}	0.37 ± 0.24^{m}
F stat	66.86 **	160.68 **	564.50 **	640.79 **	16.43 **	306.73 **	34081.04**
p value	< 0.001						
MSE	81.60	65.19	0.58	0.04	1.88	0.10	0.00
SE(m)	3.01	2.69	0.25	0.07	0.46	0.10	0.00
SE(d)	4.26	3.81	0.36	0.1	0.65	0.15	0
CV(%)	3.82	7.04	8.29	5.69	9.57	12.43	0.48
Cohen's F	3.28	5.08	9.52	10.15	1.62	7.02	74.01

Table 3: Detailed tabular representation with Multiple comparisons for Factor B. Cell values represent mean ± SDSD. Transformed means are shown in parentheses; Treatments with the same letter grouping are not significantly different; * indicates significance at 5% level; ** indicates significance at 1% level, NS indicates non-significance; MSE and CV (%) are common for this experiment.

The genotypic variation was highly significant ($p < 0.001$) for all seven traits (Table 3) and showed that there was a significant genetic variation among the 28 lentil genotypes for the root architecture and nodulation capacity. Root surface area was greatest in G1 (282.16), G7 (274.07), and G21 (268.02), and lowest in G28 (185.02) and G25 (199.02). Root volume, an important indicator of root system vigor, was greatest in G7 (26.25 cm^3), G11 (21.25 cm^3), and G5 (19.90 cm^3), and lowest in G18 (2.29 cm^3) and G3 (2.58 cm^3). The number of root nodules per plant was highest in G17 (17.22) and G7 (16.67); and lowest in G19 (10.44) and G25 (10.44); thus, G17 and G7 were categorized as being genotypes with relatively superior nodulation ability on all environments. The root total carbohydrate content was significantly higher in G7 (7.79) and G8 (6.84) than in other genotypes, with the lowest being G19 (0.34), G2 (0.67) and G28 (0.67). G25 (0.58 g), G11 (0.53 g) and G18 (0.53 g) had the highest root biomass while G1 had the lowest (0.15 g), yet it had the highest scores for RSA and RL, indicating a large but superficial root system. G7 had high values for all three parameters: RV, RN and CHO, and was a strong overall candidate to be further screened for heat-tolerance. Coefficients of variation (3.82–12.43%) and Cohen's f values (1.62–74.01) indicated good precision and moderate to very large effect sizes for the nodule number and biomass, respectively.

	RSA	RL	RV	RSD	RN	CHO	RB
E1xG1	267.29 ± 7.36^{jklmn}	191.04 ± 3.17^{ef}	8.35 ± 0.14^{rs}	2.31 ± 0.04^{xy}	25.33 ± 0.58^{defg}	2.48 ± 0.07^{jk}	0.30 ± 0.00^{D}
E1xG2	271.94 ± 2.00^{ijkl}	170.56 ± 6.29^{hij}	4.04 ± 0.15^{xyz}	1.76 ± 0.07^{zABC}	28.00 ± 2.00^{abc}	0.75 ± 0.07^{zABCDEFGH}	0.62 ± 0.00^{g}

	RSA	RL	RV	RSD	RN	CHO	RB
E1xG3	263.90 ± 8.24^{jklmno}	191.67 ± 1.30^{ef}	1.93 ± 0.01^{DEFGHIJKL}	1.12 ± 0.01^{GHIJK}	17.00 ± 0.00^{ij}	5.07 ± 0.04^{e}	0.75 ± 0.00^{b}
E1xG4	274.90 ± 12.86^{hijk}	135.60 ± 5.15^{opqr}	49.09 ± 2.42^{b}	2.84 ± 0.11^{v}	20.33 ± 1.53^{h}	1.58 ± 0.02^{pqrstuv}	0.49 ± 0.01^{o}
E1xG5	183.89 ± 1.21^{KLMNOP}	19.74 ± 0.50^{I}	47.37 ± 1.20^{c}	17.50 ± 0.44^{a}	28.33 ± 1.53^{abc}	1.57 ± 0.04^{pqrstuv}	0.44 ± 0.00^{s}
E1xG6	241.42 ± 6.85^{qrstuv}	86.18 ± 2.45^{xyzAB}	27.49 ± 0.78^{g}	7.69 ± 0.22^{j}	28.33 ± 0.58^{abc}	1.04 ± 0.02^{tuvwxyzABCD}	0.44 ± 0.00^{s}
E1xG7	321.16 ± 12.19^{ab}	49.30 ± 0.67^{H}	66.36 ± 0.90^{a}	12.90 ± 0.17^{c}	28.33 ± 3.79^{abc}	7.79 ± 0.62^{ab}	0.54 ± 0.00^{k}
E1xG8	286.62 ± 14.48^{efghi}	79.12 ± 4.80^{ABCDE}	12.90 ± 0.78^{m}	4.43 ± 0.27^{q}	27.67 ± 2.52^{abcd}	6.86 ± 0.05^{c}	0.49 ± 0.00^{p}
E1xG9	241.57 ± 4.21^{qrstuv}	117.16 ± 5.36st	8.32 ± 0.38^{rs}	2.89 ± 0.13^{v}	24.33 ± 2.08^{fg}	1.09 ± 0.02^{stuvwxyzABC}	0.40 ± 0.00^{w}
E1xG10	229.43 ± 15.46$^{uvwxyz ABC}$	63.84 ± 2.24^{EFG}	16.73 ± 0.58^{k}	5.71 ± 0.20^{n}	27.67 ± 2.08^{abcd}	2.50 ± 0.12^{jk}	0.22 ± 0.00^{H}
E1xG11	251.61 ± 8.74^{nopqrs}	16.40 ± 0.61^{I}	42.61 ± 1.59^{d}	12.56 ± 0.47^{d}	28.00 ± 2.65^{abc}	2.28 ± 0.02^{klmn}	0.76 ± 0.01^{a}
E1xG12	255.90 ± 4.38^{lmnopq}	95.64 ± 4.31^{uvwxy}	16.42 ± 0.74^{k}	4.77 ± 0.22^{pq}	26.67 ± 2.31^{bcdef}	1.79 ± 0.16^{mnopqr}	0.35 ± 0.00^{z}
E1xG13	207.40 ± 3.84^{EFGHI}	15.04 ± 0.65^{I}	34.21 ± 1.47^{e}	6.35 ± 0.27^{m}	25.67 ± 0.58^{cdef}	6.22 ± 0.09^{d}	0.42 ± 0.00^{u}
E1xG14	261.29 ± 15.57^{klmnop}	95.37 ± 1.69^{uvwxy}	30.43 ± 0.54^{f}	8.51 ± 0.15^{i}	26.33 ± 2.08^{bcdef}	2.42 ± 0.07^{jkl}	0.47 ± 0.00^{q}
E1xG15	285.41 ± 14.19^{fghi}	42.17 ± 1.70^{H}	16.91 ± 0.68^{k}	7.05 ± 0.29^{l}	27.00 ± 1.00^{bcde}	1.17 ± 0.04^{rstuvwxyzABC}	0.55 ± 0.01^{j}
E1xG16	196.23 ± 2.80^{IJKLMN}	115.20 ± 1.76st	12.40 ± 0.19^{m}	3.65 ± 0.06^{rst}	30.00 ± 3.61^{a}	1.18 ± 0.02^{rstuvwxyzAB}	0.35 ± 0.00^{z}
E1xG17	242.27 ± 9.56^{qrstuv}	127.38 ± 7.98^{rs}	3.69 ± 0.23^{yzAB}	8.22 ± 0.52^{i}	29.00 ± 1.73^{ab}	0.81 ± 0.03^{yzABCDEFGH}	0.53 ± 0.00^{l}
E1xG18	242.55 ± 6.47^{qrstuv}	125.03 ± 3.86^{rs}	1.74 ± 0.05^{FGHIJKLM}	1.31 ± 0.04^{EFGH}	26.67 ± 2.52^{bcdef}	4.17 ± 0.07^{f}	0.69 ± 0.00^{c}
E1xG19	181.76 ± 4.23^{LMNOP}	84.85 ± 4.39^{xyzAB}	5.57 ± 0.29^{uvw}	2.87 ± 0.15^{v}	14.00 ± 1.73^{lmno}	0.82 ± 0.02^{yzABCDEFGH}	0.57 ± 0.00^{i}
E1xG20	215.27 ± 13.42$^{zABCD EFGH}$	92.67 ± 5.71^{vwxyzA}	2.47 ± 0.15$^{ABCDEFGH I}$	1.79 ± 0.11^{zABC}	23.00 ± 1.73^{g}	2.89 ± 0.05^{ij}	0.60 ± 0.00^{h}
E1xG21	318.99 ± 11.87^{ab}	179.43 ± 7.59^{fgh}	0.80 ± 0.03^{JKLM}	0.74 ± 0.03^{JKLM}	25.67 ± 1.15^{cdef}	3.91 ± 0.05^{fg}	0.65 ± 0.00^{e}
E1xG22	278.87 ± 13.84^{ghij}	13.22 ± 0.26^{I}	23.72 ± 3.50^{h}	14.23 ± 0.65^{b}	24.67 ± 0.58^{efg}	3.75 ± 0.07^{fg}	0.44 ± 0.00^{s}
E1xG23	290.31 ± 2.46^{efgh}	103.64 ± 0.88^{tuvw}	16.73 ± 2.94^{k}	9.25 ± 0.08^{gh}	23.00 ± 2.00^{g}	3.74 ± 0.02^{fg}	0.44 ± 0.00^{s}
E1xG24	232.82 ± 8.85^{tuvwxyz}	83.12 ± 3.16^{xyzAB}	16.51 ± 1.01^{k}	7.42 ± 0.28^{jk}	15.33 ± 1.53^{jkl}	4.09 ± 0.08^{fg}	0.32 ± 0.00^{B}
E1xG25	187.80 ± 3.44^{JKLMNO}	67.96 ± 0.52^{CDEF}	11.68 ± 0.17^{mn}	6.07 ± 0.05^{m}	14.33 ± 2.08^{klmn}	4.04 ± 0.08^{fg}	0.65 ± 0.00^{e}
E1xG26	239.43 ± 3.86^{qrstuvw}	81.36 ± 3.13^{yzABC}	15.95 ± 1.00^{k}	7.26 ± 0.28^{kl}	14.67 ± 0.58^{jklm}	2.04 ± 0.05^{klmnop}	0.43 ± 0.00^{t}
E1xG27	184.94 ± 10.11$^{KLMNO P}$	17.42 ± 0.67^{I}	19.38 ± 1.52^{j}	8.95 ± 0.39^{h}	18.00 ± 1.00^{i}	1.06 ± 0.02^{tuvwxyzABCD}	0.54 ± 0.00^{k}
E1xG28	186.27 ± 4.27^{KLMNOP}	17.80 ± 1.03^{I}	14.17 ± 0.81^{l}	11.76 ± 0.68^{e}	26.67 ± 1.53^{bcdef}	0.44 ± 0.08^{DEFGH}	0.60 ± 0.00^{h}
E2xG1	267.38 ± 10.11^{jklmn}	260.95 ± 7.19^{b}	1.66 ± 0.05^{FGHIJKLM}	0.91 ± 0.01^{HIJKLM}	9.67 ± 0.58^{stuvwx}	1.88 ± 0.09^{lmnopq}	0.12 ± 0.00^{Q}
E2xG2	165.07 ± 1.21^{Q}	96.98 ± 0.71^{uvwxy}	3.48 ± 0.03^{yzABC}	2.14 ± 0.10^{xyz}	10.67 ± 0.58^{qrstuv}	0.40 ± 0.03^{EFGH}	0.51 ± 0.00^{n}
E2xG3	214.80 ±	145.80 ±	1.55 ±	1.13 ±	11.33 ±	4.98 ± 0.02^{e}	0.31 ±

	RSA	RL	RV	RSD	RN	CHO	RB
	6.71^{ABCDEFGH}	4.55^{mnop}	0.05^{FGHIJKLM}	0.05^{GHIJ}	0.58^{opqrst}		0.00^{C}
E2xG4	187.57 ± 8.77^{JKLMNO}	43.50 ± 2.03^{H}	1.08 ± 0.05^{GHIJKLM}	1.00 ± 0.03^{HIJKLM}	10.67 ± 1.15^{qrstuv}	1.53 ± 0.00^{pqrstuvw}	0.36 ± 0.00^{y}
E2xG5	270.07 ± 2.45^{ijklm}	131.87 ± 0.87^{pqr}	10.95 ± 0.07^{no}	3.29 ± 0.09^{tu}	13.33 ± 1.53^{lmnop}	1.57 ± 0.00^{pqrstuv}	0.32 ± 0.00^{B}
E2xG6	252.57 ± 7.17^{nopqrs}	86.81 ± 2.46^{xyzAB}	3.40 ± 0.09^{yzABCD}	2.22 ± 0.03^{xy}	14.33 ± 0.58^{klmn}	1.67 ± 0.00^{opqrst}	0.32 ± 0.00^{B}
E2xG7	302.01 ± 11.47^{cde}	83.56 ± 3.18^{xyzAB}	9.99 ± 0.38^{opq}	3.91 ± 0.09^{r}	13.67 ± 1.53^{lmno}	7.36 ± 0.98^{bc}	0.42 ± 0.00^{u}
E2xG8	274.97 ± 13.89^{hijk}	18.18 ± 0.92^{I}	4.68 ± 0.24^{wxy}	0.97 ± 0.05^{HIJKLM}	7.00 ± 0.00^{xyzABCDE}	6.83 ± 0.04^{c}	0.43 ± 0.00^{t}
E2xG9	220.64 ± 3.85^{xyzABCDEF}	79.34 ± 1.39^{zABCDE}	0.37 ± 0.01^{M}	0.76 ± 0.06^{IJKLM}	9.33 ± 1.53^{stuvwxy}	1.01 ± 0.02^{uvwxyzABCDE}	0.21 ± 0.00^{I}
E2xG10	240.96 ± 16.24^{qrstuv}	148.25 ± 9.99^{lmno}	1.07 ± 0.07^{GHIJKLM}	1.45 ± 0.07^{CDEFG}	9.33 ± 0.58^{stuvwxy}	2.33 ± 0.00^{jklm}	0.21 ± 0.00^{I}
E2xG11	234.67 ± 8.16^{stuvwxy}	133.61 ± 4.64^{opqr}	20.74 ± 0.72^{i}	1.53 ± 0.03^{CDEF}	11.00 ± 0.00^{pqrstu}	1.63 ± 0.04^{opqrstu}	0.65 ± 0.00^{e}
E2xG12	252.21 ± 4.31^{nopqrs}	224.19 ± 3.83^{d}	2.58 ± 0.05^{ABCDEFG}	1.25 ± 0.05^{EFGH}	13.00 ± 1.73^{lmnopq}	1.43 ± 0.17^{pqrstuvwxy}	0.32 ± 0.00^{B}
E2xG13	237.68 ± 4.40^{rstuvwx}	85.26 ± 1.58^{xyzAB}	2.54 ± 0.05^{ABCDEFGH}	1.94 ± 0.14^{yzAB}	10.33 ± 0.58^{rstuvw}	5.78 ± 0.19^{d}	0.41 ± 0.00^{v}
E2xG14	265.46 ± 15.82^{jklmn}	160.69 ± 9.58^{ijkl}	1.15 ± 0.07^{GHIJKLM}	0.96 ± 0.05^{HIJKLM}	14.33 ± 0.58^{klmn}	2.22 ± 0.19^{klmno}	0.32 ± 0.00^{B}
E2xG15	200.14 ± 9.96^{GHIJK}	88.34 ± 4.40^{wxyzAB}	4.03 ± 0.20^{xyz}	2.46 ± 0.05^{wx}	13.67 ± 0.58^{lmno}	1.00 ± 0.00^{vwxyzABCDE}	0.45 ± 0.00^{r}
E2xG16	241.09 ± 3.44^{qrstuv}	65.70 ± 0.94^{DEF}	6.39 ± 0.09^{tuv}	3.61 ± 0.24^{rst}	11.67 ± 1.53^{nopqrs}	0.87 ± 0.09^{xyzABCDEFG}	0.21 ± 0.00^{I}
E2xG17	169.37 ± 6.68^{PQ}	50.52 ± 1.99^{GH}	5.27 ± 0.21^{vwx}	3.73 ± 0.24^{r}	15.00 ± 0.00^{jklm}	0.67 ± 0.00^{ABCDEFGH}	0.52 ± 0.00^{m}
E2xG18	219.93 ± 5.87^{yzABCDEF}	88.20 ± 2.35^{wxyzAB}	2.96 ± 0.08^{zABCDEF}	2.03 ± 0.04^{yzA}	16.67 ± 2.08^{ijk}	1.63 ± 2.14^{opqrstu}	0.45 ± 0.00^{r}
E2xG19	213.39 ± 4.96^{BCDEFGHI}	68.01 ± 1.58^{CDEF}	8.41 ± 0.38^{rs}	5.38 ± 0.15^{no}	12.67 ± 2.52^{lmnopqr}	0.63 ± 0.04^{BCDEFGH}	0.47 ± 0.00^{q}
E2xG20	245.30 ± 15.29^{pqrstu}	67.13 ± 4.18^{CDEF}	7.60 ± 0.87st	5.08 ± 0.23^{op}	12.33 ± 1.53^{mnopqr}	2.63 ± 0.04^{ijk}	0.42 ± 0.00^{u}
E2xG21	230.89 ± 8.59^{tuvwxyzAB}	46.49 ± 1.73^{H}	14.50 ± 1.28^{l}	9.51 ± 0.37^{g}	14.00 ± 1.00^{lmno}	3.67 ± 0.00^{fgh}	0.54 ± 0.00^{k}
E2xG22	215.49 ± 10.69^{zABCDEFGH}	137.91 ± 6.85^{nopqr}	9.27 ± 0.46^{pqr}	2.97 ± 0.09^{uv}	15.33 ± 1.53^{jkl}	3.86 ± 0.16^{fg}	0.31 ± 0.00^{C}
E2xG23	221.57 ± 1.88^{xyzABCDEF}	258.52 ± 2.19^{b}	3.32 ± 0.03^{yzABCDE}	1.32 ± 0.09^{DEFGH}	14.33 ± 0.58^{klmn}	0.93 ± 0.04^{wxyzABCDEF}	0.21 ± 0.00^{I}
E2xG24	197.98 ± 7.52^{HIJKLM}	162.15 ± 6.16^{ijkl}	5.41 ± 0.20^{vwx}	2.01 ± 0.06^{yzA}	14.00 ± 1.00^{lmno}	3.93 ± 0.04^{fg}	0.23 ± 0.00^{G}
E2xG25	198.99 ± 3.64^{GHIJKL}	158.93 ± 2.91^{jklm}	2.19 ± 0.04^{CDEFGHIJK}	1.99 ± 0.07^{yzAB}	9.00 ± 1.00^{tuvwxyz}	3.18 ± 1.31^{hi}	0.45 ± 0.00^{r}
E2xG26	196.73 ± 3.16^{IJKLMN}	110.04 ± 1.77^{tu}	6.38 ± 0.11^{tuv}	2.72 ± 0.12^{vw}	11.67 ± 0.58^{nopqrs}	1.76 ± 0.19^{mnopqr}	0.31 ± 0.00^{C}
E2xG27	204.00 ± 11.16^{FGHIJ}	233.48 ± 43.96^{cd}	6.49 ± 0.36^{tuv}	1.62 ± 0.07^{BCDE}	12.33 ± 0.58^{mnopqr}	1.87 ± 0.14^{lmnopq}	0.31 ± 0.00^{C}
E2xG28	188.24 ± 4.32^{JKLMNO}	129.72 ± 2.97^{qrs}	0.39 ± 0.01^{M}	0.63 ± 0.01^{M}	11.67 ± 1.53^{nopqrs}	0.37 ± 0.04^{FGH}	0.45 ± 0.00^{r}
E3xG1	311.81 ± 8.58^{abc}	99.07 ± 2.72^{uvwx}	1.00 ± 0.01^{IJKLM}	1.11 ± 0.02^{GHIJKL}	6.00 ± 1.00^{ABCDE}	1.47 ± 0.14^{pqrstuvwx}	0.02 ± 0.00^{V}

	RSA	RL	RV	RSD	RN	CHO	RB
E3xG2	211.12 ± 1.56^{DEFGHI}	116.57 ± 0.86st	4.31 ± 0.19^{wxyz}	2.22 ± 0.08^{xy}	6.67 ± 1.53^{yzABCDE}	0.27 ± 0.04^{GH}	0.09 ± 0.00^{R}
E3xG3	247.89 ± 7.74^{opqrst}	200.00 ± 13.35^{e}	4.27 ± 0.16^{wxyz}	1.69 ± 0.05^{ABCD}	7.00 ± 1.00^{xyzABCDE}	4.88 ± 0.08^{e}	0.24 ± 0.00^{F}
E3xG4	308.87 ± 14.45^{bcd}	92.15 ± 8.53^{vwxyzA}	3.77 ± 0.13^{yzA}	1.15 ± 0.07^{FGHI}	8.67 ± 1.15^{uvwxyzA}	1.56 ± 0.05^{pqrstuv}	0.23 ± 0.00^{G}
E3xG5	176.40 ± 1.16^{OPQ}	185.09 ± 1.22^{fg}	1.39 ± 0.04^{GHIJKLM}	0.97 ± 0.05^{HIJKLM}	7.33 ± 0.58^{xyzABCDE}	1.52 ± 0.02^{pqrstuvw}	0.67 ± 0.01^{d}
E3xG6	272.23 ± 7.73^{ijkl}	170.21 ± 4.83^{hij}	3.02 ± 0.05^{zABCDEF}	1.47 ± 0.10^{CDEFG}	5.67 ± 0.58^{BCDE}	1.54 ± 0.08^{pqrstuvw}	0.09 ± 0.01^{S}
E3xG7	199.05 ± 7.56^{GHIJKL}	296.94 ± 11.28^{a}	2.39 ± 0.06^{ABCDEFGHI}	1.07 ± 0.05^{GHIJKL}	8.00 ± 1.00^{wxyzABC}	8.21 ± 0.08^{a}	0.13 ± 0.01^{P}
E3xG8	239.85 ± 12.11^{qrstuvw}	243.36 ± 12.30^{c}	8.81 ± 0.44^{qrs}	2.09 ± 0.01^{xyz}	6.67 ± 0.58^{yzABCDE}	6.83 ± 0.04^{c}	0.29 ± 0.00^{E}
E3xG9	250.87 ± 4.38^{nopqrs}	135.24 ± 2.36^{opqr}	1.29 ± 0.11^{GHIJKLM}	1.10 ± 0.02^{GHIJKL}	8.33 ± 0.58^{vwxyzAB}	0.87 ± 0.09^{xyzABCDEFG}	0.17 ± 0.00^{N}
E3xG10	215.95 ± 14.56^{zABCDEFG}	93.19 ± 6.28^{vwxyzA}	0.44 ± 0.02^{LM}	0.72 ± 0.07^{JKLM}	6.00 ± 1.00^{ABCDE}	1.70 ± 0.24^{nopqrs}	0.39 ± 0.00^{x}
E3xG11	294.59 ± 10.23^{defg}	96.11 ± 3.34^{uvwxy}	0.41 ± 0.01^{LM}	0.72 ± 0.02^{KLM}	6.67 ± 0.58^{yzABCDE}	1.54 ± 0.08^{pqrstuvw}	0.18 ± 0.00^{L}
E3xG12	225.80 ± 3.86^{vwxyzABCD}	67.44 ± 1.15^{CDEF}	0.56 ± 0.02^{LM}	0.99 ± 0.02^{HIJKLM}	7.67 ± 0.58^{xyzABCD}	5.77 ± 0.17^{d}	0.20 ± 0.00^{J}
E3xG13	216.47 ± 4.01^{zABCDEFG}	75.00 ± 1.39^{BCDE}	6.84 ± 0.50^{tu}	3.34 ± 0.11st	6.33 ± 0.58^{zABCDE}	2.21 ± 0.08^{klmno}	0.03 ± 0.00^{U}
E3xG14	230.38 ± 13.73^{tuvwxyzAB}	42.28 ± 2.52^{H}	0.72 ± 0.04^{KLM}	0.70 ± 0.05^{LM}	4.67 ± 0.58^{E}	0.86 ± 0.06^{xyzABCDEFG}	0.18 ± 0.01^{M}
E3xG15	222.87 ± 11.08^{wxyzABCDE}	95.18 ± 4.73^{uvwxyz}	2.28 ± 0.05^{BCDEFGHIJ}	1.78 ± 0.08^{zABC}	6.00 ± 0.00^{ABCDE}	0.83 ± 0.04^{yzABCDEFG}	0.13 ± 0.01^{P}
E3xG16	197.19 ± 2.81^{IJKLMN}	66.95 ± 0.96^{CDEF}	0.40 ± 0.02^{LM}	0.84 ± 0.05^{IJKLM}	5.33 ± 0.58^{CDE}	0.54 ± 0.08^{CDEFGH}	0.15 ± 0.00^{O}
E3xG17	325.36 ± 12.83^{a}	180.41 ± 18.95^{fgh}	4.76 ± 0.31^{wxy}	1.12 ± 0.03^{GHIJK}	7.67 ± 0.58^{xyzABCD}	3.88 ± 0.21^{fg}	0.52 ± 0.00^{m}
E3xG18	232.35 ± 6.20^{tuvwxyzA}	174.83 ± 4.66^{ghi}	2.18 ± 0.04^{CDEFGHIJK}	1.26 ± 0.01^{EFGH}	5.00 ± 0.00^{DE}	3.85 ± 0.14^{fg}	0.45 ± 0.00^{r}
E3xG19	272.72 ± 6.34^{ijkl}	104.89 ± 7.14^{tuv}	2.17 ± 0.06^{CDEFGHIJK}	0.78 ± 0.02^{IJKLM}	4.67 ± 1.53^{E}	0.54 ± 0.05^{CDEFGH}	0.22 ± 0.00^{H}
E3xG20	212.51 ± 13.24^{CDEFGHI}	192.75 ± 36.94^{ef}	1.87 ± 0.09^{EFGHIJKLM}	0.63 ± 0.04^{M}	8.67 ± 0.58^{uvwxyzA}	2.60 ± 0.09^{jk}	0.39 ± 0.00^{x}
E3xG21	254.18 ± 9.46^{mnopqr}	39.39 ± 1.47^{H}	8.52 ± 1.10^{rs}	9.99 ± 0.79^{f}	6.00 ± 1.00^{ABCDE}	3.61 ± 0.02^{fgh}	0.34 ± 0.00^{A}
E3xG22	300.20 ± 14.89^{cdef}	88.88 ± 4.41^{wxyzAB}	8.56 ± 0.55^{rs}	5.03 ± 0.18^{p}	5.67 ± 1.53^{BCDE}	3.53 ± 0.04^{gh}	0.35 ± 0.00^{z}
E3xG23	237.67 ± 2.02^{rstuvwx}	164.01 ± 1.39^{ijk}	10.34 ± 0.82^{op}	4.53 ± 0.15^{q}	7.00 ± 0.00^{xyzABCDE}	0.82 ± 0.02^{yzABCDEFGH}	0.32 ± 0.00^{B}
E3xG24	246.37 ± 9.36^{pqrstu}	290.07 ± 11.02^{a}	7.69 ± 0.63st	2.44 ± 0.18^{wx}	6.33 ± 0.58^{zABCDE}	3.78 ± 0.05^{fg}	0.03 ± 0.00^{U}
E3xG25	210.27 ± 3.85^{DEFGHI}	142.99 ± 2.62^{nopq}	1.53 ± 0.05^{FGHIJKLM}	1.16 ± 0.02^{FGHI}	8.00 ± 1.00^{wxyzABC}	1.27 ± 0.09^{qrstuvwxyzA}	0.64 ± 0.00^{f}
E3xG26	179.72 ± 2.89^{NOPQ}	132.77 ± 2.14^{pqr}	1.02 ± 0.05^{HIJKLM}	1.01 ± 0.03^{HIJKLM}	8.67 ± 0.58^{uvwxyzA}	1.34 ± 0.29^{qrstuvwxyz}	0.19 ± 0.00^{K}
E3xG27	246.30 ± 13.47^{pqrstu}	151.53 ± 8.28^{klmn}	1.39 ± 0.06^{GHIJKLM}	1.07 ± 0.02^{GHIJKL}	5.00 ± 0.00^{DE}	0.87 ± 0.09^{xyzABCDEFG}	0.52 ± 0.00^{m}
E3xG28	180.55 ±	53.86 ±	5.60 ±	3.66 ±	7.00 ±	0.21 ± 0.05^{H}	0.07 ±

	RSA	RL	RV	RSD	RN	CHO	RB
	4.14^{MNOPQ}	1.24^{FGH}	0.08^{uvw}	0.03^{rs}	$0.00^{xyzABCDE}$		0.00^{T}
F stat	47.54 **	191.04 **	485.37 **	611.09 **	17.00 **	24.48 **	13838.48 **
p value	< 0.001						
MSE	81.60	65.19	0.58	0.04	1.88	0.10	0.00
SE(m)	5.22	4.66	0.44	0.12	0.79	0.18	0.00
SE(d)	7.38	6.59	0.62	0.17	1.12	0.26	0
CV (%)	3.82	7.04	8.29	5.69	9.57	12.43	0.48
Cohen's F	3.91	7.84	12.49	14.02	2.34	2.80	66.69

Table 4: Detailed tabular representation with Multiple comparisons for Interaction AxB. Cell values represent mean ± SDSD. Transformed means are shown in parentheses; Treatments with the same letter grouping are not significantly different; * indicates significance at 5% level; ** indicates significance at the 1% level, NS indicates non-significance; MSE and CV (%) are common for this experiment.

For all traits, the genotype × environment interaction was highly significant ($p < 0.001$) (Table 4), which indicated that the interaction of genotype with temperature for the two fields (E2 and E3) and the offspring (E1) was not consistent—genotypes that were best in E1 were not necessarily best in E2 or E3. This is especially important for the number of nodules as heat-induced suppression of nodulation could vary between different genotypes, and hence some genotypes may be more heat tolerant than others with respect to the ability to sustain nodulation under delayed sowing conditions, which has direct relevance in selecting heat-resilient, symbiotically stable genotypes. Genotype × environment interaction was detected for all traits resulting in Cohen's f values between 2.34 and 66.69, being most pronounced for root biomass.

Figure 1 shows generally weak to moderate relationships between the seven root and nodulation traits tested when performed on a Pearson correlation basis.There were also positive correlations between root volume and root surface diameter (r = 0.59) and root nodule number (r = 0.27) to a lesser degree, and with root total carbohydrate (r = 0.32).The root surface area had moderate positive correlation with root total carbohydrate (r = 0.45) and weak positive correlation with root nodule number (r = 0.32) and root volume (r = 0.30).There were negative correlations between root length and root surface diameter (r = −0.28), root volume (r = −0.21), and root nodule number (r = −0.20), which indicated that the genotypes with greater root length tended to have lower root surface diameter, lower root volume, and fewer root nodules.Generally the correlations of root biomass with the other traits were weak (+/−0.18 to 0.23).

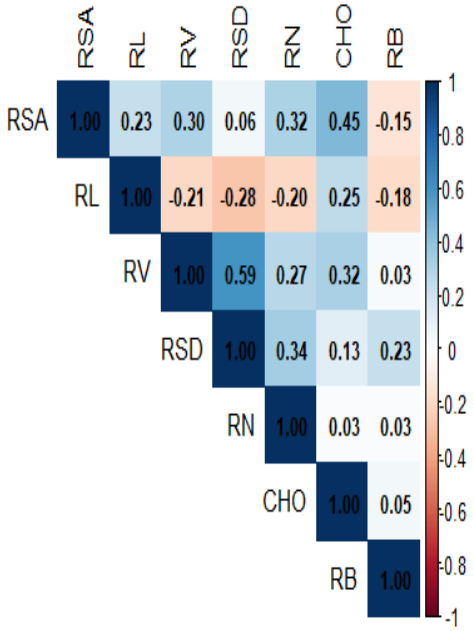

Figure 1. Pearson correlation heatmap among root and nodulation traits.

Principal component analysis extracted five components, of which the first two accounted for 55.1% of the total variance (PC1 = 31.2%, PC2 = 23.9%; Table 5, Figure 2). PC3, PC4, and PC5 explained an additional 14.9%, 11.4%, and 8.3%, respectively, together bringing the cumulative variance explained by the first five components to 89.7%.

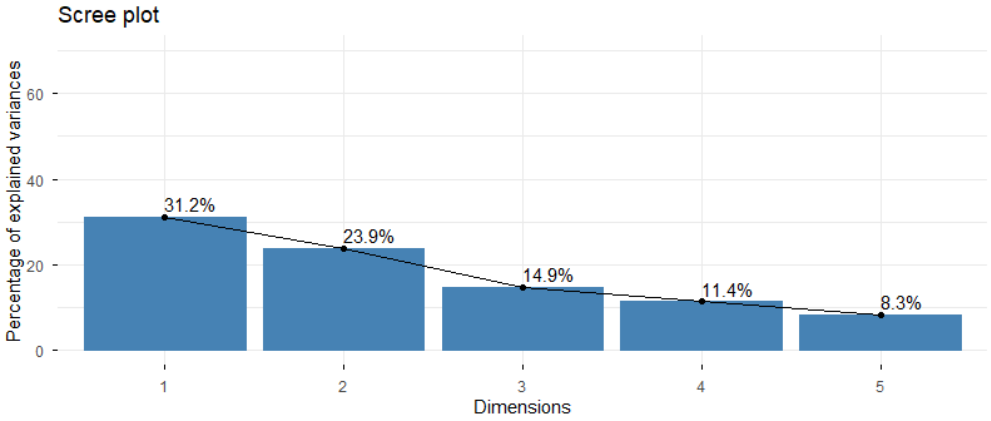

Figure 2. Scree plot of percentage variance explained by each principal component.

The root length loading was negatively weighted while root biomass was moderately positively weighted, and root surface diameter and root volume were most strongly positively weighted by PC1 (0.873 and 0.847, respectively); root nodule number was positively weighted (0.793). As a result, RSD, RV and RN were the greatest contributors to PC1 (26.8%, 25.2% and 22.1% of its variance, respectively; Table 6, Figure 3), which defined PC1 as a general "root vigor–nodulation" axis opposed by root elongation. Root total carbohydrate (0.762) and root surface area (0.759) accounted for 84.1% of the variance of PC2 and were the dominant variables, forming a distinct axis very different from PC1 and a "surface area – carbohydrate reserve" axis. The highest-quality representation (cos^2) was for root surface diameter (0.77) and root volume (0.73), and the lowest for root biomass (0.34; Figure 4); RB's variance is best represented on the PC1–PC2 plane, and is well captured by later components (notably PC3, where RB loads 0.715 and contributes 57.0% of PC3's variance).

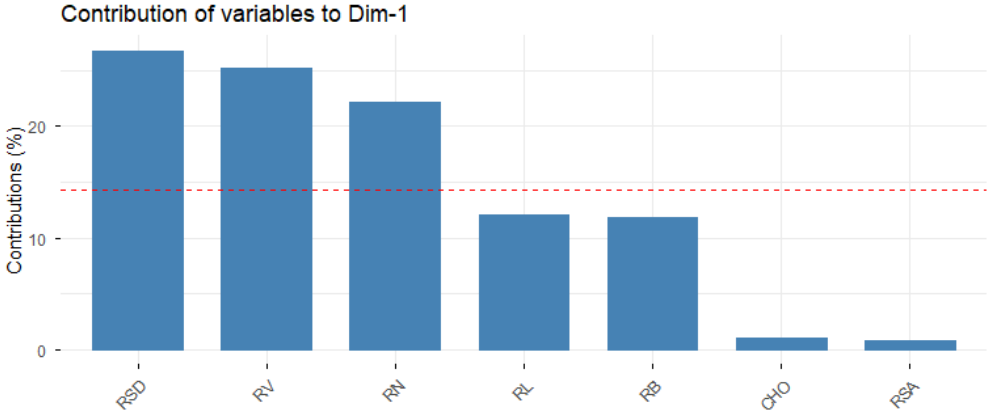

Figure 3. Percentage contribution of each trait to Principal Component 1.

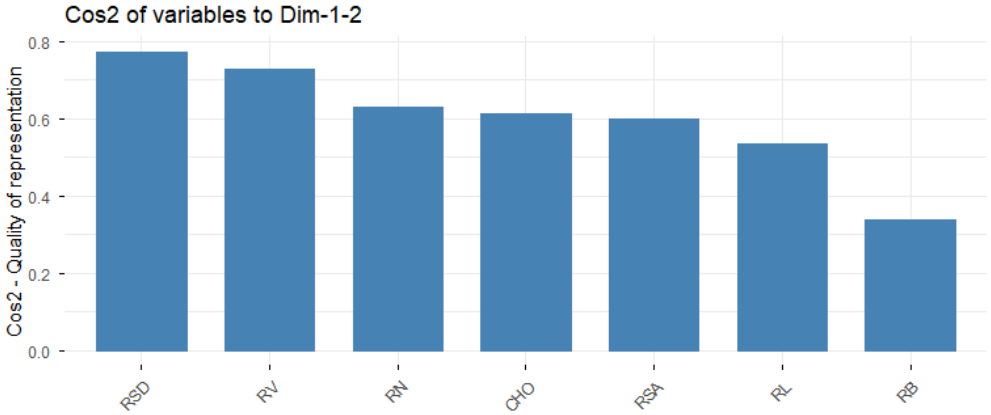

Figure 4. Quality of representation (cos^2) of variables on the PC1–PC2 plane.

Ordination of traits and genotypes

The variable correlation circle and PCA biplot revealed that root volume, root surface diameter and root number of nodules vectors aligned in the same direction along PC1, indicating that these variables are positively correlated with each other, whereas root length vector is in the opposite direction, suggesting the trade-off between root growth in length and increment in thickness/nodulation/root volume as observed in the correlation

matrix (Figure 5a and 5b). The root surface area and root total carbohydrate vectors were more closely correlated along PC2 than along PC1 cluster of traits. The distribution of individual observations on PC1 (Figure 6) revealed a group of high-scoring observations clearly segregated from the main body, suggesting genotypes that produce significantly more root volume, diameter and nodulation in specific genotype x environment combinations than other observations.

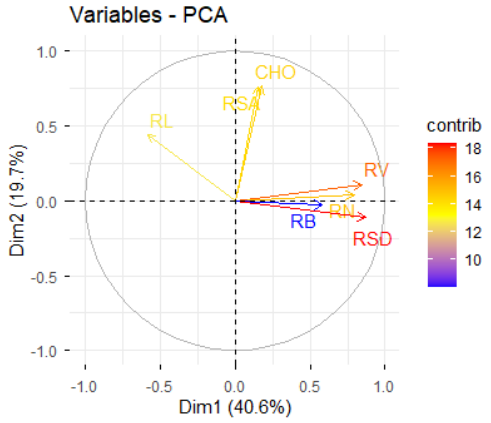

Figure 5a. Variable correlation circle showing trait vectors on the PC1–PC2 plane.

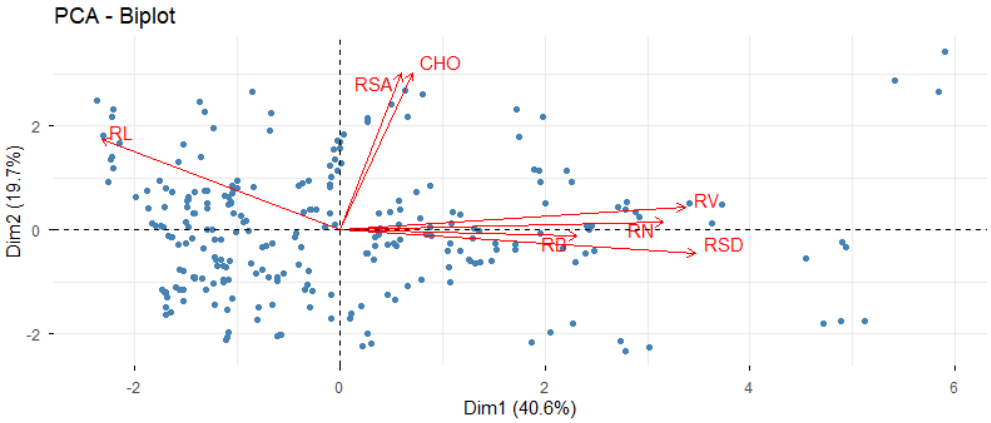

Figure 5b. PCA biplot of individual observations and trait vectors.

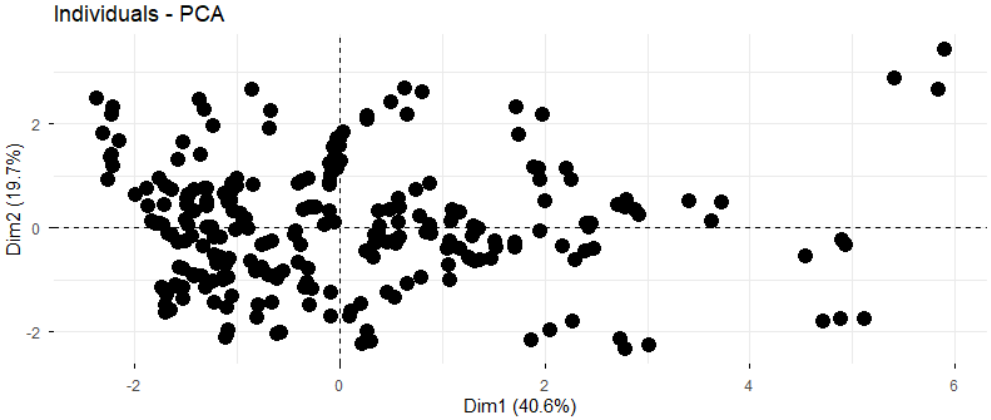

Figure 6. Distribution of individual observations on the PC1–PC2 plane.

The 28 genotypes were classified into four major clusters with hierarchical cluster analysis (Figure 7). Cluster I comprised genotypes G3, G14, G15, G24, and G26; Cluster II comprised G1, G16, G17, G22, and G27; Cluster III comprised G11, G18, G19, G20, and G21; and Cluster IV, the largest, comprised G2, G4, G5, G6, G7, G8, G9, G10, G12, G13, G23, G25, and G28. The heatmap-based clustering of standardized trait means (Figure 8) confirmed the opposite variation of root volume and root surface diameter, as well as the correlation and PCA results, with this grouping of traits showing a generally similar variation across genotypes; root nodule number was a relatively distinct group from the RV–RSD group. The partitioning of trait correlations into direct and indirect effects is shown in Figure 9, which uses root biomass (RB) as the dependent variable with path analysis. Root nodule number (RN) had the highest direct positive path coefficient (0.49) for root biomass (RB), such that nodulation was the most important direct factor contributing to biomass accumulation in this trait network. Root volume (RV) did not have a significant direct effect on RB (0.02), but had a strong indirect effect, through root nodule number ($0.57 \times 0.49 \approx 0.28$). The direct impact of Root Surface Area (RSA) on RB had a small negative

value (−0.10), but it was largely offset by its direct contribution to RV (0.20 × 0.28 ≈ 0.06), bringing the overall direct impact of RSA to near neutral (0.10).

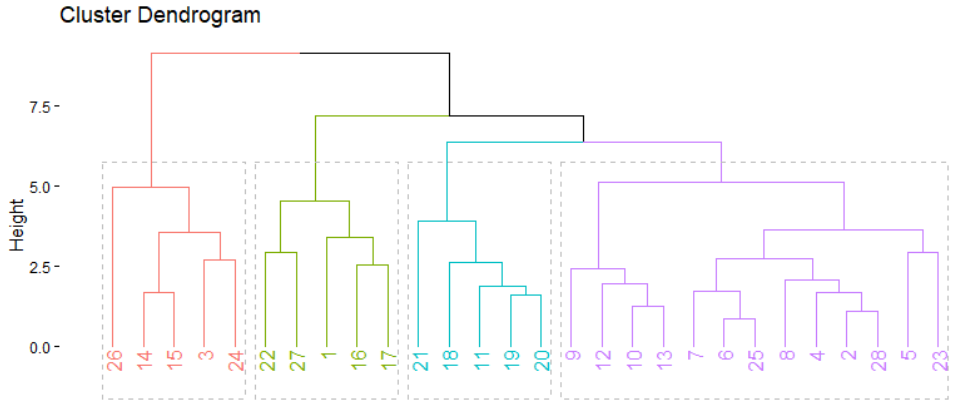

Figure 7. Dendrogram of hierarchical clustering of 28 lentil genotypes based on root and nodulation traits.

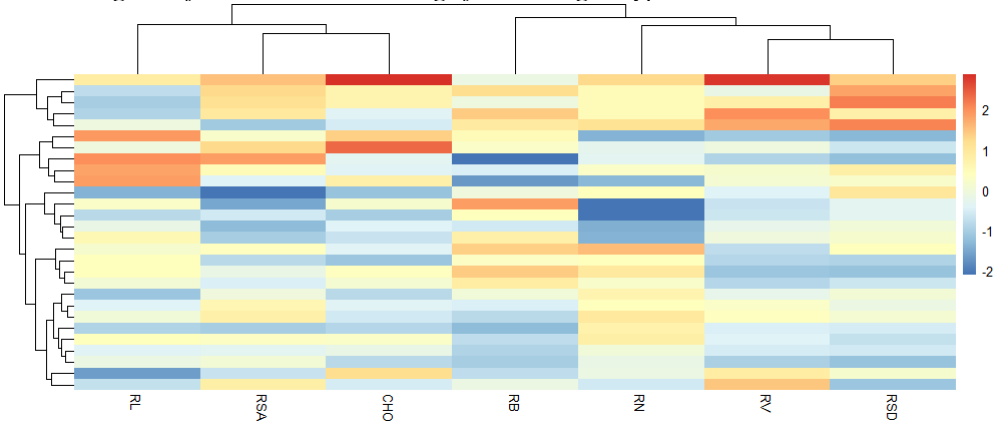

Figure 8. Heatmap of standardized trait means with hierarchical clustering of genotypes and traits.

Root length (RL) was not directly related to RB, but it negatively influenced RB indirectly through RV (path coefficient RL→RV = −0.38) which in turn had a negative effect on RN (path coefficient RV→RN = −0.57), and hence indirectly on RB (path coefficient RL→RV→RN = −0.57 × −0.38 = −0.11). This is the inverse link revealed in the correlation and PCA analysis between root length and root vigor that were carried out to the final outcome, which was a lower amount of root biomass in genotypes that had invested massively in root elongation. Root volume was also directly correlated with root surface diameter (0.75) and root total carbohydrate (CHO = 0.23), making root volume a central hub trait connecting root architecture with both structural and biochemical root traits. A negative residual correlation (−0.07) between root nodule number and root total carbohydrate and a small positive residual correlation (0.03) between RSD and RB suggested that there was some remaining unaccounted covariation associated with this relationship that was not included in the assumed causal paths. Overall, the path analysis supports the idea that root nodule number is the major direct limiting factor in this genotype set, and that, in turn, is mainly limited by root volume, which confirms the high priority of root nodule number for indirect selection for increased root biomass under heat stress.

Figure 9. Path diagram showing direct (arrows) and residual (curved lines) effects of root traits on root biomass.

4. DISCUSSION

The significant reduction in the number of root nodules under delayed sowing conditions (E2, E3) compared to the timely sown control (E1) is consistent with the well-documented thermal sensitivity of the legume–rhizobium symbiosis. A comparable pattern of nodulation loss under heat stress has been reported in pea, where prolonged exposure to elevated temperature triggered an unusual apical pattern of nodule senescence and degradation of symbiotic structures, with recovery possible only if the stress episode was short (Serova et al., 2023). Work with common bean-nodulating *Rhizobium* strains has similarly shown that heat exposure impairs symbiotic nitrogen fixation and cell survival even in strains selected for heat tolerance, indicating that the rhizobial partner, and not only the host plant, contributes to symbiotic thermotolerance (Michiels et al., 1994). The optimal temperature range for nodulation and nitrogen fixation in most legumes is generally considered to lie between approximately 20 and 30 °C, with nodule initiation delayed below this range and nodule structure and function impaired above it (Sindhu et al., 2020), consistent with the progressive decline in nodule number

observed here as the sowing date, and hence the temperature experienced during the reproductive stage, was pushed later.

The genotypic variation in nodule number observed in this study, together with the pronounced genotype × environment interaction, indicates that some lentil genotypes (G17 and G7) sustain nodulation more effectively than others under heat stress. This agrees with the broader recognition that the legume–rhizobium symbiosis is not a fixed, temperature-dependent trait but one shaped jointly by host and microsymbiont responses to abiotic stress (Hawkins & Oresnik, 2022). Genotypes such as G7, which combined comparatively high root volume, nodule number, and carbohydrate content across environments, are therefore reasonable candidates for further evaluation as sources of stable symbiotic performance under heat stress.

The compensatory increase in root length, occurring alongside reductions in root volume, nodule number, and carbohydrate content, is consistent with a foraging-type response in which the plant redirects resources away from radial thickening and nodulation and toward exploring a larger soil volume as thermal, and presumably moisture, stress intensifies (Koevoets et al., 2016). This trade-off parallels the broader distinction between root ideotypes optimised for rapid, low-cost soil exploration and those optimised for resource-rich, metabolically "expensive" growth (Lynch, 2013); the shift toward longer, thinner, less nodulated roots under heat stress observed here can be read as a shift away from a root-vigour/nodulation economy and toward an exploratory one. A comparable plasticity in root length and diameter under abiotic stress has been documented across lentil germplasm evaluated for drought tolerance, where genotypic differences in root architecture were closely linked to differences in stress survival (Priya et al., 2021), suggesting that root-length plasticity is a general component of the lentil stress-response repertoire rather than one specific to heat.

These results are reinforced by the multivariate analyses. Root volume, surface diameter, and nodule number formed a coherent trait complex (PC1) opposed by root elongation, whereas surface area and carbohydrate reserves defined an independent axis (PC2), suggesting that root vigour/nodulation and root surface area/carbohydrate economy vary largely independently within this genotype set and could, in principle, be selected separately without negative trade-offs(Aktar-Uz-Zaman et al., 2022). The path analysis further indicated that root nodule number was the most important direct determinant of root biomass, with root volume acting as its main upstream driver; this places root nodule number, rather than root length or surface area alone, as the more useful indirect selection criterion under heat-stressed sowing conditions. Hierarchical clustering broadly reproduced this grouping by nodulation performance, and the co-clustering of the two highest-nodulating genotypes, G7 and G17, offers a practical basis for choosing genetically distinct parents for future heat-tolerance breeding crosses.

A few caveats deserve mention. The heat-stress gradient in this study was generated through delayed sowing at a single location and season, so temperature was confounded with associated changes in day length, radiation, and residual soil moisture (Sadras et al., 2015); multi-location and multi-year testing, together with direct canopy or soil temperature records, would help isolate a purely thermal effect from these co-varying factors. Nodule function (nitrogenase activity, leghemoglobin content) was not measured directly in this study, so the extent to which reduced nodule number under heat stress reflects impaired initiation versus accelerated senescence, as described for pea (Serova et al., 2023), remains to be established for lentil specifically.

5. CONCLUSIONS

Terminal heat stress substantially reduced root volume, root diameter, carbohydrate content, and nodulation in lentil, while promoting compensatory root elongation. The magnitude of genotypic variability and the significant genotype × environment interaction observed across all seven traits indicate that lentil germplasm harbours diverse strategies for coping with heat stress at the root and nodulation level, rather than a single uniform response. Root volume, root diameter, carbohydrate status, and nodulation emerged as the most heat-responsive and mechanistically informative traits in this trait network, with nodule number identified as the strongest direct determinant of root biomass and root volume as its main upstream driver. Genotypes combining favourable performance across these traits, such as G7 and G17, represent useful starting material for breeding programmes targeting climate-resilient lentil cultivars, and the selection framework developed here, prioritising root volume, root diameter, carbohydrate content, and nodule number as an indirect selection index, could be extended to other short-duration pulses facing similar terminal heat stress. Confirming these trait relationships across additional environments and seasons, and linking them to nodule-level physiological measurements, would strengthen their use as selection criteria in applied breeding programmes.

6. ACKNOWLEDGEMENTS

The authors sincerely acknowledge the financial support provided by Dr. Rajendra Prasad Central Agricultural University for carrying out this research work under the university-funded research project.

7. Conflict of Interest

The authors declare no conflict of interest.

8. Author Contributions

Jyostnarani Pradhan: Conceptualization, methodology, investigation, data analysis, and manuscript preparation. **Chandani Kumari, Hemlata Singh, Swati Bhimrao Gaikwad, and Ravi Pakash:** Investigation

and data collection. **Kshirod Chandra Sahoo and Shiv Nath Suman:** Methodology, investigation, and technical support. **Kartik Pramanik:** Conceptualization, supervision, data analysis, and manuscript review and editing.

9. REFERENCES

Aktar-Uz-Zaman, M., Haque, M. A., Sarker, A., Alam, M. A., Rohman, M. M., Ali, M. O., Alkhateeb, M. A., Gaber, A., & Hossain, A. (2022). Selection of Lentil (*Lens Culinaris* (Medik.)) Genotypes Suitable for High-Temperature Conditions Based on Stress Tolerance Indices and Principal Component Analysis. *Life*, *12*(11), 1719. https://doi.org/10.3390/life12111719

Choukri H, El Haddad N, Aloui K, Hejjaoui K, El-Baouchi A, Smouni A, Thavarajah D, Maalouf F and Kumar S (2022) Effect of High Temperature Stress During the Reproductive Stage on Grain Yield and Nutritional Quality of Lentil (*Lens culinaris* Medikus). Front. Nutr. 9:857469. doi: 10.3389/fnut.2022.857469

Hawkins, J. P., & Oresnik, I. J. (2022). The Rhizobium-legume symbiosis: co-opting successful stress management. *Frontiers in Plant Science*, 12, 796045.

Koevoets, I. T., Venema, J. H., Elzenga, J. T. M., & Testerink, C. (2016). Roots withstanding their environment: Exploiting root system architecture responses to abiotic stress to improve crop tolerance. Frontiers in Plant Science, 7, 1335. https://doi.org/10.3389/fpls.2016.01335

Luo, H., Xu, H., Chu, C., He, F., & Fang, S. (2020). High temperature can change root system architecture and intensify root interactions of plant seedlings. *Frontiers in plant science*, *11*, 160.

Lynch, J. P. (2013). Steep, cheap and deep: an ideotype to optimize water and N acquisition by maize root systems. *Annals of Botany*, 112(2), 347–357.

Lynch, J. P. (2022). Harnessing root architecture to address global challenges. *The Plant Journal*, *109*(2), 415-431.

Michiels, J., Verreth, C., & Vanderleyden, J. (1994). Effects of temperature stress on bean-nodulating Rhizobium strains. *Applied and Environmental Microbiology*, 60(4), 1206–1212.

Priya, S., Bansal, R., Kumar, G., Dikshit, H. K., Kumari, J., Pandey, R., Singh, A. K., Tripathi, K., Singh, N., Kumari, N. K. P., Kumar, S., & Kumar, A. (2021). Root trait variation in lentil (*Lens culinaris* Medikus) germplasm under drought stress. *Plants*, 10(11), 2410.

Sadras, V. O., Vadez, V., Purushothaman, R., Lake, L., & Marrou, H. (2015). Unscrambling confounded effects of sowing date trials to screen for crop adaptation to high temperature. Field Crops Research, 177, 1–8. https://doi.org/10.1016/j.fcr.2015.02.024

Serova, T. A., Kusakin, P. G., Kitaeva, A. B., Seliverstova, E. V., Gorshkov, A. P., Romanyuk, D. A., ... & Tsyganov, V. E. (2023). Effects of elevated temperature on Pisum sativum nodule development: I—Detailed characteristic of unusual apical senescence. *International Journal of Molecular Sciences*, *24*(24), 17144.

Sindhu, S., Dahiya, A., Gera, R., & Sindhu, S. S. (2020). Mitigation of abiotic stress in legume-nodulating rhizobia for sustainable crop production. *Agricultural Research*, 9(4), 444–459.

Sita, K., Sehgal, A., Bhandari, K., Kumar, J., Kumar, S., Singh, S., Siddique, K. H. M., & Nayyar, H. (2018). Impact of heat stress during seed filling on seed quality and seed yield in lentil (*Lens culinaris* Medikus) genotypes. Journal of the Science of Food and Agriculture, 98(13), 5134–5141. https://doi.org/10.1002/jsfa.9054

11. Supplementary Material

The influence of high temperature stress on root structure in word file is given in the supplementary material.

The influence of high-temperature stress on root structure

IPL329			IPL225		
					
E1	E2	E3	E1	E2	E3
IPL220			IPL406		

					
E1	E2	E3	E1	E2	E3
IPL321			IPL526		
					
E1	E2	E3	E1	E2	E3
IPL230			IPL315		
					
E1	E2	E3	E1	E2	E3
IPL81			IPL316		
					
E1	E2	E3	E1	E2	E3
IPL341			IPL534		
					
E1	E2	E3	E1	E2	E3
PANT-L-9			PANT 117		

					
E1	E2	E3	E1	E2	E3
PUSA AGETI			PL-7		
					
E1	E2	E3	E1	E2	E3
PSL 9			DPL15		
					
E1	E2	E3	E1	E2	E3
DPL62			KSL 218		
					
E1	E2	E3	E1	E2	E3
HUL 57			VL 148		
					
E1	E2	E3	E1	E2	E3
L 4727			L4602		

					
E1	E2	E3	E1	E2	E3
L-9-12			LL1698		
					
E1	E2	E3	E1	E2	E3
LL1694			LL1641		
					
E1	E2	E3	E1	E2	E3